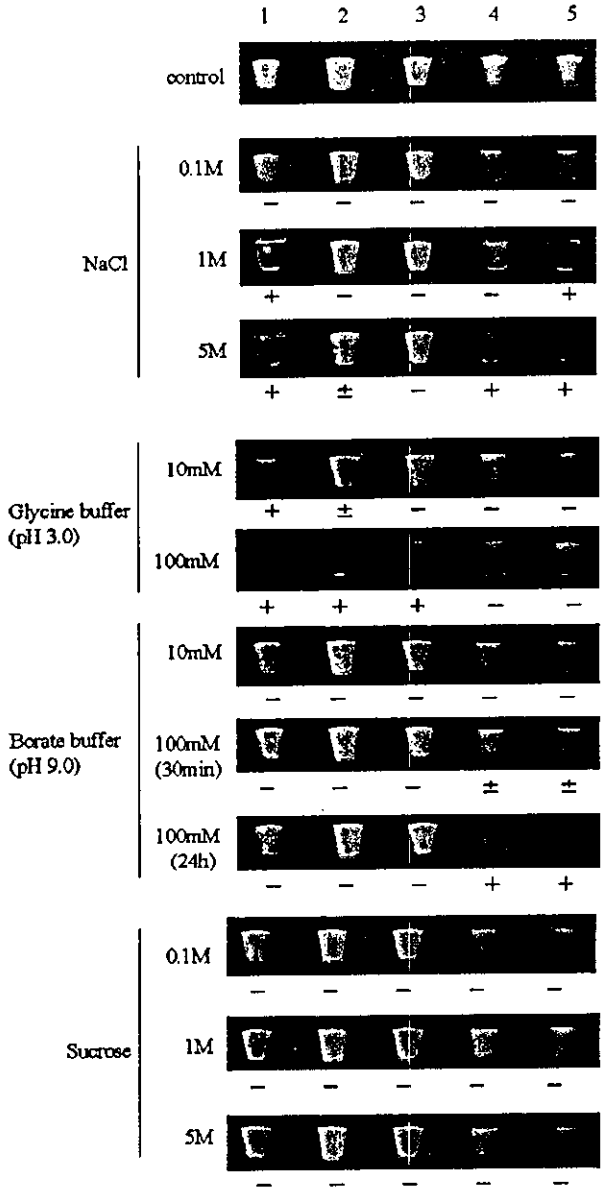

Figure 3. Physicochemical stability of various modified QDs in aqueous buffers. A QD aqueous solution (10 μM) was diluted by the indicated buffers (QD final concentration 100 nM), and incubated for 30 min at room temp. The snapshots were captured using a digital camera with $^1/_{30}$ s exposure excited by a 365-nm wavelength (UV-A). The results were reproduced in three separate experiments. 1, QD-COOH; 2, QD-OH/COOH; 3, QD-OH, 4, QD-NH_2/OH; 5, QD-NH_2; +, aggregated; ±, partially aggregated; −, not aggregated.

cytometry (Figure 5). QDs were introduced into cells by an endocytotic mechanism by adding culture media.[14,25] Cell death was observed by adding crude QDs. In contrast, low cell damage and high labeling efficiency were achieved by adding purified QDs. However, slight cell death was observed only by purified QD-COOH. This cytotoxicity may be caused by uptake QDs located in endosomes.[14] As surface molecules were bound to QDs through the electric interaction

Table 1. DNA-Damaging Effects of the Ingredients and Impurities of the QD Samples

compound	dose (μg/mL)	tail length of 50 nuclei (mm, mean ⊥ SE) 2-h treatment	12-h treatment
MUA	0	23.4 ± 1.05	23.9 ± 1.21
	25	25.6 ⊥ 0.58	28.1 ⊥ 1.31
	50	33.8 ± 2.38[a]	41.2 ± 3.31[a]
	100	54.6 ± 3.27[a]	toxic
	200	76.0 ± 3.52[a]	toxic
	400	80.3 + 3.18[a]	toxic
cysteamine	0	23.5 ⊥ 0.81	24.1 ⊥ 1.05
	50	22.4 ± 0.40	25.1 ± 1.12
	100	23.4 ± 0.95	29.6 ± 1.72
	200	22.9 ± 0.90	35.4 ± 2.89[a]
	400	23.3 ± 0.82	44.5 ± 2.21[a]
thioglycerol	0	23.5 ± 0.81	24.1 ± 1.05
	50	24.7 ± 1.06	27.0 ± 1.65
	100	26.0 ± 1.28	24.7 ± 1.24
	200	22.4 + 0.83	24.6 + 0.99
	400	23.4 ⊥ 0.98	28.1 ⊥ 1.84
TOPO	0	23.8 ± 0.91	23.1 ± 1.04
	50	24.9 ± 0.47	22.5 ± 0.56
	100	27.1 ± 1.33	26.3 ± 1.81
	200	29.6 + 1.92	28.1 + 1.33
	400	32.5 ± 1.43[a]	31.7 ± 1.31[a]
ZnS	0	23.8 ± 0.91	23.1 ± 1.04
	50	23.7 ± 0.89	24.1 ± 0.51
	100	22.5 ± 0.53	22.4 ± 0.34
	200	24.1 ⊥ 0.71	24.1 ⊥ 0.56
	400	23.3 ± 0.54	22.2 ± 0.97

[a] $P < 0.05$.

between the sulfhydryl group and QD-covered zinc,[25] surface molecules such as MUA may be detached by acidic and oxidative conditions in endosomes and released into cytoplasm.[34] The fluorescence of QDs was lost by low pH, by oxidation of the surface structures, or by some intracellular factors adsorbed onto QDs,[13] implying that the advanced development of the surface modification of QDs needs to overcome the cytotoxicity. However, this detachment could be utilized to release valuable materials such as medicines and genes into cells by cellular oxidative/reductive conditions.

Next, to investigate whether cell death by QDs was carried out by an apoptotic pathway, we evaluated the genotoxic potential of QDs by comet assay with WTK1 cells.[27-29] A significant increase in the tail length was observed after 2 h of treatment with QD-COOH at 2 μM (Figure 6a). After treatment for 12 h, the tail length was equal to that of the control cells, suggesting that the induced DNA damage was efficiently repaired during prolonged incubation. Crude QD-COOH samples prepared by only membrane filtration, but not by ultrafiltration, showed stronger DNA damage than purified QD-COOH (Figure 6b). However, QD-NH2, QD-OH, QD-OH/COOH, and QD-NH2/OH induced no DNA damage up to a dose of 4 μM for 2 h. To determine whether the genotoxicity of QDs was caused by QD particles themselves, three ingredients of the QD samples (MUA, cysteamine, and thioglycerol) and two possible impurities (TOPO and ZnS) were also assayed. As shown

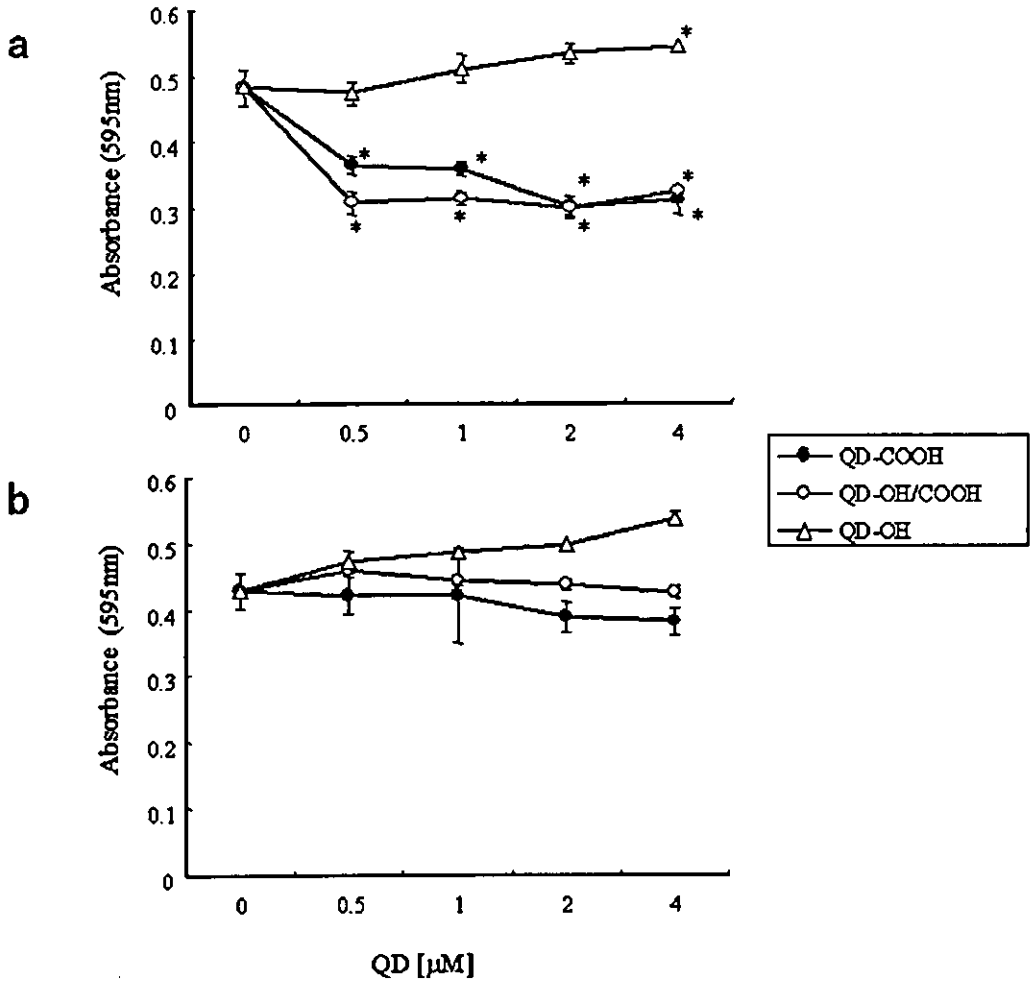

Figure 4. Contaminated impurities and ingredients in QD samples suppress the proliferation of cultured cells. Vero cells were plated at 5×10^4 cells on 96-well plates and cultured for 4 h with (a) crude QD and (b) ultrafiltartion-purified QDs in coexisting MTT reagents (Roche Diagnostics). After incubation, the cells were lysed on the plate, and 595-nm absorbance (reduced hormazan) was measured with a microplate reader. Data are presented as the mean ± standard deviation of duplicate samples. Significance was evaluated by the *t* test versus negative control. *, $p < 0.05$.

in Table 1, treatment with MUA for 12 h caused severe cytotoxicity at doses greater than 100 μg/mL (approximately coordinated to 4μM QD-COOH). DNA damage was observed at doses greater than or equal to 50 μg/mL with 2 h of treatment. Cysteamine was weakly genotoxic when cells were treated for 12 h. Thioglycerol was negative in the assay, suggesting that QD-OH was the least toxic QD among them. Because TOPO was also found to be a cytotoxic and genotoxic compound, the complete removal of TOPO from the QD samples is important in reducing toxicity. These results provided evidence that some hydrophilic compound-coated QDs are responsible for the genotoxicity of QD. Almost all of the DNA damage induced by QD-COOH was efficiently repaired in the cells because DNA damage detected by the comet assay did not persist in the cells treated for 12 h. However, the possibility remains that a few nonrepaired DNA lesions can result in gene mutations or chromosome aberrations. These results provided evidence that some hydrophilic compound-coated QDs are responsible for the cytotoxicity of QDs. It is an important factor for designing less-toxic QDs to select hydrophilic compounds to dissolve QDs in water. These results suggested that the surface treatment of nanocrystals (surface-covered functional groups and biomolecules covered the surface of QDs) has specified the biological behavior of whole nanocrystal QDs.

Nanocrystal QDs have the great potential to be applied to molecular biology and bioimaging because of several advantages over organic fluorophores. As of now, the potential toxicity of industrial products is not considered, whereas the pharmaceutical preparations cannot be commercialized without strictly investigating detrimental effect to human, resulting in the environmental pollution that was caused by the leakage of toxic substance from scrapped industrial products. We the manufacturers must be responsible for characterizing the potential environmental effects and biological toxicity of novel nanomaterial products for industrial laborers and consumers before products are widely

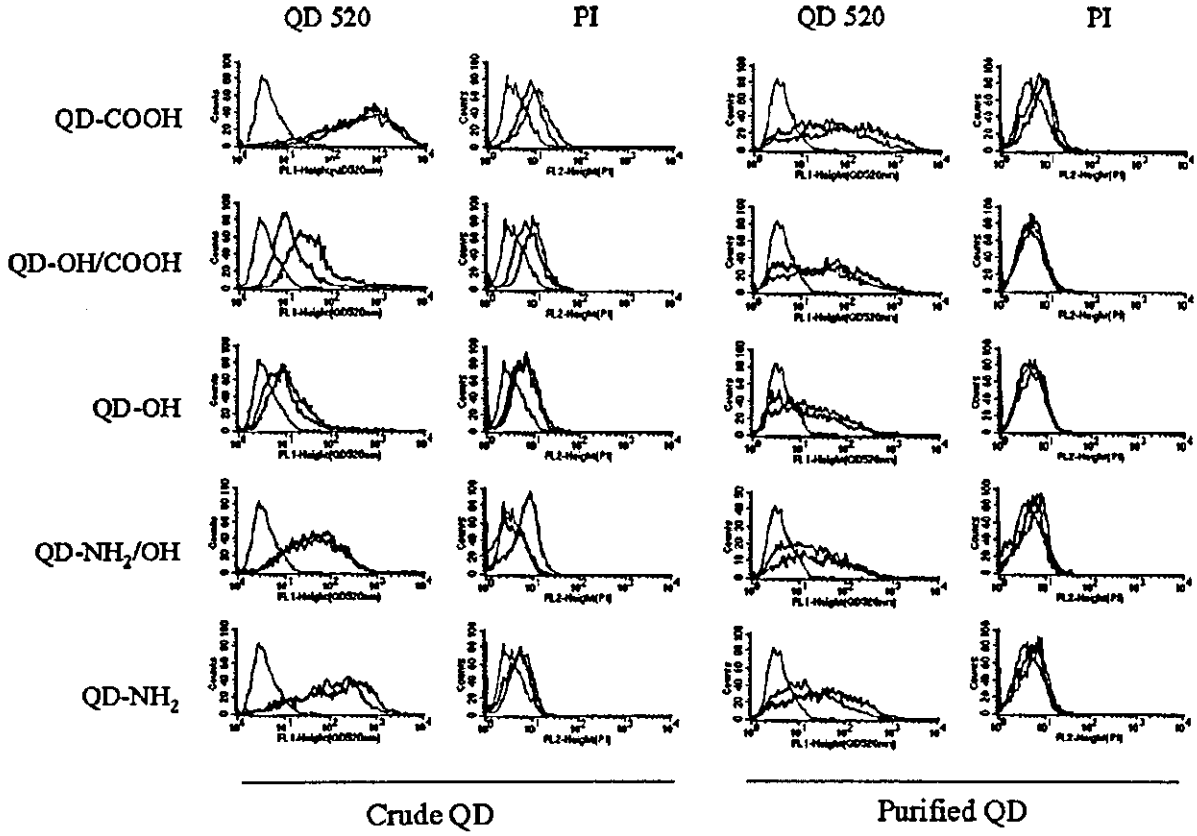

Figure 5. Contaminated impurities and ingredients in QD samples induce cell death. Vero cells were plated at 1×10^5 cells on 24-well plate and incubated for 12 h with crude QDs and ultrafiltration-purified QDs at 2 μM (red line) and 1 μM (blue line). Then cells were harvested, stained with propidium iodide, and analyzed by flow cytometry. The x axis indicates the fluorescence intensity of QDs (left columns) and PI (right columns) on a log scale. The green line shows untreated cells as a negative control. Results are representative of three separate experiments.

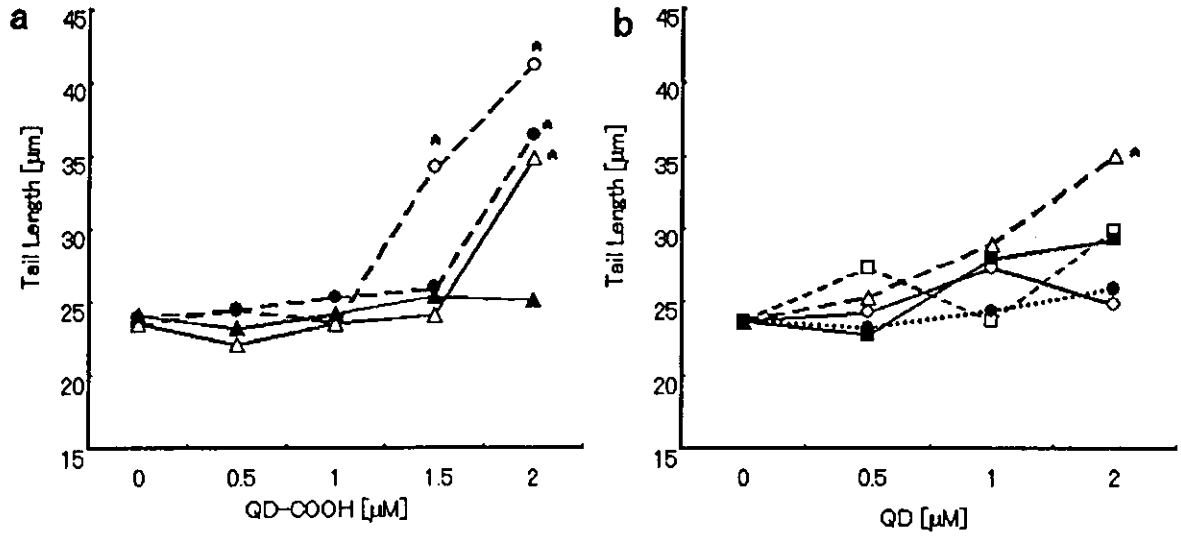

Figure 6. DNA-damaging effects of hydrophilic nanocrystalline QDs by comet assay. (a) WTK-1 cells were treated with QD-COOH (ultrafiltration purified; ▲, △) or QD-COOH (crude; ●, ○) for 2 h (open symbols) and 12 h (filled symbols). Then cells were harvested and embedded in 1% agarose, and electrophoresis was performed at 0 °C for 20 min at 25 V (0.96 V/cm) and approximately 250 mA. After being stained with ethidium bromide, the length of the whole comet was measured for 50 nuclei for each dose using a fluorescence microscope (200× magnification). (b) Cells were treated with QD-COOH (△), QD-NH_2 (□), QD-OH (○), QD-OH/COOH (●), or QD-NH_2/OH (■) for 2 h. The difference between the means in the treated and control plates was compared with the Dunnett test after one-way ANOVA. *, $p < 0.05$.

commercialized. In this paper, we revealed that the toxicity of QDs in biological systems is not dependent on the nanocrystal particle itself but on the surface molecules. In the case of QDs, no cytotoxicity was detected from their ingredients or the QD core itself, suggesting that surface processing will overcome the toxicity of nanomaterials. Less cytotoxicity derived from their ingredients or the QD core itself was observed in QD-OH in vitro. It is expected that QDs will be applied in the biomedical field for the innovative investigation, diagnosis, and medical treatment of various diseases.[9-12] When producing nanometer-sized materials in the future, it will be vital that the behavior of QDs in the biological system is not dependent on the chemical properties of surface-covered molecules but on the nanocrystalline particle itself. Surface modifications of functional molecules combined with nanoparticles may work as bionanomachines conforming to the functions designated by their surface molecules.

We conclude that the surface treatment of nanocrystals (surface-covered functional groups and biomolecules covering the surface of QDs) has specified the biological behavior of whole nanocrystalline QDs. We hope that the surface modifications of functional molecules combined with nanoparticles may work as a bionanomachine conforming to the functions designated by their surface molecules.

Acknowledgment. We are grateful to Dr. Akira Yuo and Dr. Taeko Dohi (Research Institute, IMCJ) for generously providing valuable advice about data collection. We thank Dr. Yukio Yamaguchi and colleagues (Department of Chemical System Engineering, University of Tokyo) for amino-QD improvements. This work was supported by a Medical Techniques Promotion Research Grant from the Ministry of Health, Labor and Welfare of Japan (H14-nano-004).

Supporting Information Available: Experimental procedures: Preparation of CdSe/ZnS fluorescent nanocrystal Qdots, preparation of surface-modified nanocrystal QDs, and protocols for comet assay and cell viability assays. This material is available free of charge via the Internet at http://pubs.acs.org.

References

(1) Colvin, V. L. *Nat. Biotechnol.* **2003**, *21*, 1166−1170.
(2) Borm, P. J. *Inhalation Toxicol.* **2002**, *14*, 311−324.
(3) Albrecht, C.; Borm, P. J.; Adolf, B.; Timblin, C. R.; Mossman, B. T. *Toxicol. Appl. Pharmacol.* **2002**, *184*, 37−45.
(4) Schins, R. P.; Duffin, R.; Hohr, D.; Knaapen, A. M.; Shi, T.; Weishaupt, C.; Stone, V.; Donaldson, K.; Borm, P. J. *Chem. Res. Toxicol.* **2002**, *15*, 1166−1173.
(5) Rosenthal, S. J.; Tomlinson, I.; Adkins, E. M.; Schroeter, S.; Adams, S.; Swafford, L.; McBride, J.; Wang, Y.; DeFelice, L. J.; Blakely, R. D. *J. Am. Chem. Soc.* **2002**, *124*, 4586−4594.
(6) Dubertret, B.; Skourides, P.; Norris, D. J.; Noireaux, V.; Brivanlou, A. H.; Libchaber, A. *Science* **2002**, *298*, 1759−1762.
(7) Jaiswal, J. K.; Mattoussi, H.; Mauro, J. M.; Simon, S. M. *Nat. Biotechnol.* **2003**, *21*, 47−51.
(8) Xu, H.; Sha, M. Y.; Wong, E. Y.; Uphoff, J.; Xu, Y.; Treadway, J. A.; Truong, A.; O'Brien, E.; Asquith, S.; Stubbins, M.; Spurr, N. K.; Lai, E. H.; Mahoney, W. *Nucleic Acids Res.* **2003**, *31*, 43.
(9) Wu, X.; Liu, H.; Liu, J.; Haley, K. N.; Treadway, J. A.; Larson, J. P.; Ge, N.; Peale, F.; Bruchez, M. P. *Nat. Biotechnol.* **2003**, *21*, 41−46.
(10) Chan, W. C.; Maxwell, D. J.; Gao, X.; Bailey, R. E.; Han, M.; Nie, S. *Curr. Opin. Biotechnol.* **2002**, *13*, 40−46.
(11) Zhu, L.; Ang, S.; Liu, W. T. *Appl. Environ. Microbiol.* **2004**, *70*, 597−598.
(12) Mattoussi, H.; Mauro, J. M.; Goldman, E. R.; Anderson, G. P.; Sundar, V. C.; Mikulec F. V.; Bawendi, M. G. *J. Am. Chem. Soc.* **2000**, *122*, 12142−12150.
(13) Gerion, D.; Pinaud, F.; Williams, S. C.; Parak, W. J.; Zanchet, D.; Weiss, S.; Alivisatos, A. P. *J. Phys. Chem. B* **2001**, *105*, 8861−8871.
(14) Hanaki, K.; Momo, A.; Oku, T.; Komoto, T.; Maenosono, S.; Yamaguchi, Y.; Yamamoto, K. *Biochem. Biophys. Res. Commun.* **2003**, *302*, 496−501.
(15) Medintz, I. L.; Clapp, A. R.; Mattoussi, H.; Goldman, E. R.; Fisher, B.; Mauro, J. M. *Nat. Mater.* **2003**, *9*, 630−638.
(16) Chan, W. C.; Nie, S. *Science* **1998**, *281*, 2016−2018.
(17) Goldman, E. R.; Balighian, E. D.; Mattoussi, H.; Kuno, M. K.; Mauro, J. M.; Tran, P. T.; Anderson, G. P. *J. Am. Chem. Soc.* **2002**, *124*, 6378−6382.
(18) Gao, X.; Chan, W. C.; Nie, S. *J. Biomed. Opt.* **2002**, *7*, 532−537.
(19) Akerman, M. E.; Chan, W. C.; Laakkonen, P.; Bhatia, S. N.; Ruoslahti, E. *Proc. Natl. Acad. Sci. U.S.A.* **2002**, *99*, 12617−12621.
(20) Larson, D. R.; Zipfel, W. R.; Williams, R. M.; Clark, S. W.; Bruchez, M. P.; Wise, F. W.; Webb, W. W. *Science* **2003**, *300*, 1434−1436.
(21) Mansson, A.; Sundberg, M.; Balaz, M.; Bunk, R.; Nicholls, I. A.; Omling, P.; Tagerud, S.; Montelius, L. *Biochem. Biophys. Res. Commun.* **2004**, *314*, 529−534.
(22) Pellegrino, T.; Parak, W. J.; Boudreau, R.; LeGros, M. A.; Gerion, D.; Alivisatos, A. P.; Larabell, C. A. *Differentiation* **2003**, *71*, 542−548.
(23) Levene, M. J.; Dombeck, D. A.; Kasischke, K. A.; Molloy, R. P.; Webb, W. W. *J. Neurophysiol.* **2004**, *91*, 1908−12.
(24) Dahan, M.; Levi, S.; Luccardini, C.; Rostaing, P.; Riveau, B.; Triller, A. *Science* **2003**, *302*, 442−445.
(25) Hoshino, A.; Hanaki, K.; Suzuki, K.; Yamamoto, K. *Biochem. Biophys. Res. Commun.* **2004**, *314*, 46−53.
(26) Singh, N. P.; McCoy, M. T.; Tice, R. R.; Schneider, E. L. *Exp. Cell. Res.* **1988**, *175*, 184−191.
(27) Sasaki, Y. F.; Tsuda, S.; Izumiyama, F.; Nishidate, E. *Mutat. Res.* **1997**, *388*, 33−44.
(28) Sasaki, Y. F.; Sekihashi, K.; Izumiyama, F.; Nishidate, E.; Saga, A.; Ishida, K.; Tsuda, S. *Crit. Rev. Toxicol.* **2000**, *30*, 629−799.
(29) Tice, R. R.; Agurell, E.; Anderson, D.; Burlinson, B.; Hartmann, A.; Kobayashi, H.; Miyamae, Y.; Rojas, E.; Ryu, J. C.; Sasaki, Y. F. *Environ. Mol. Mutagen.* **2000**, *35*, 206−221.
(30) Hines, M. A.; Guyot-Sionnest, P. *J. Phys. Chem.* **1996**, *100*, 468−471.
(31) Dabboussi, B. O.; Rodriguez-Viejo, J.; Mikulec, F. V.; Heine, J. R.; Mattoussi, H.; Ober, R.; Jensen, K. F.; Bawendi, M. G. *J. Phys. Chem. B* **1997**, *101*, 9463−9475.
(32) Reynolds, C. P.; Biedler, J. L.; Spengler, B. A.; Reynolds, D. A.; Ross, R. A.; Frenkel, E. P. *J. Natl Cancer Inst.* **1986**, *76*, 375−87.
(33) Liber, H. L.; Yandell, D. W.; Little, J. B. *Mutat. Res.* **1989**, *216*, 9−17.
(34) Bruchez, M., Jr.; Moronne, M.; Gin, P.; Weiss, S.; Alivisatos, A. P. *Science* **1998**, *281*, 2013−2016.

NL048715D

IMMUNOPHARMACOLOGY AND IMMUNOTOXICOLOGY
Vol. 26, No. 4, pp. 527–543, 2004

Induction of Coronary Arteritis with Administration of CAWS (*Candida albicans* Water-Soluble Fraction) Depending on Mouse Strains

Noriko Nagi-Miura,[1] Yuko Shingo,[1] Yoshiyuki Adachi,[1] Akiko Ishida-Okawara,[2] Toshiaki Oharaseki,[3] Kei Takahashi,[3] Shiro Naoe,[3] Kazuo Suzuki,[2] and Naohito Ohno, Ph.D.[1,*]

[1]Laboratory for Immunopharmacology of Microbial Products, School of Pharmacy, Tokyo University of Pharmacy and Life Science, Hachioji, Tokyo, Japan
[2]Department of Bioactive Molecules, National Institute of Infectious Diseases, Tokyo, Japan
[3]Department of Pathology, Ohashi Hospital, Toho University School of Medicine, Tokyo, Japan

ABSTRACT

The intraperitoneal administration of CAWS (water-soluble extracellular polysaccharide fraction obtained from the culture supernatant of *Candida albicans*) to mice induces coronaritis similar to Kawasaki disease. We analyzed differences in the production of cytokines involved in the occurrence of coronary arteritis among mouse strains, C3H/HeN, C57BL/6, DBA/2 and CBA/J that were injected with CAWS at 4 mg/mouse for 5 consecutive days in the first week and the fifth week of administration. The incidence of arteritis was 100% in C57BL/6, C3H/HeN and DBA/2 mice, but only 10% in CBA/J mice. The coronary arteritis observed in DBA/2 mice

*Correspondence: Prof. Naohito Ohno, Ph.D., Laboratory for Immunopharmacology of Microbial Products, School of Pharmacy, Tokyo University of Pharmacy and Life Science, 1432-1, Horinouchi, Hachioji, Tokyo 192-0392, Japan; Fax: 81-426-76-5570; E-mail: ohnonao@ps.toyaku.ac.jp.

DOI: 10.1081/IPH-200042295
0892-3973 (Print); 1532-2513 (Online)

was the most serious, with several mice expiring during the observation period. The CAWS-sensitive strains revealed increased levels of IL-6 and IFN-γ during the course of a specific response to CAWS by spleen cells. In contrast, IL-10 levels were observed to increase markedly in CAWS-resistant CBA/J mice, but not the CAWS-sensitive strains. However, TNF-α levels were more elevated only in DBA/2 mice. The difference in disease development and cytokine production strongly suggests that the genetic background of the immune response to CAWS contributes to the occurrence of coronary arteritis.

Key Words: *Candida albicans*; Induction of arteritis; Polysaccharide; DBA/2 mice.

INTRODUCTION

Kawasaki disease, also referred to as acute febrile mucocutaneous lymph node syndrome or MCLS, was first reported by Kawasaki in 1967.[1,2] A disease of unknown cause, it affects mainly children aged 4 and under. The number of patients diagnosed with Kawasaki disease annually is roughly 10,000. The patients present with systemic coronary arteritis, and the greatest concern with this symptom is the occurrence of coronary arteritis or coronaritis, which occurs as a sequela in nearly 10% of all patients.[3,4] Moreover, in the case of the formation of giant coronary aneurysms, complications involving myocardial ischemia and myocardial disorders caused by vascular occlusion due to thrombus formation may arise. In actuality, sudden death due to myocardial infarction occurs in several percent of Kawasaki disease patients. Although the occurrence of such coronary artery disorders has decreased with the introduction of γ-globulin therapy, the mechanism of their occurrence along with the pharmacological mechanism of the treatment is unknown.[5,6]

Murata et al.[7,8] reported that Kawasaki-disease-like coronary arteritis was induced specifically at the origin of the coronary arteries in mice administered an alkaline extract of *C. albicans* isolated from patients (CADS) with Kawasaki disease. Ishida-Okawara et al.[9] have demonstrated that mice with coronary arthritis induced with a CADS injection show an increase in anti-myeloperoxidase (MPO)-specific anti-neutrophil cytoplasmic antibody (MPO-ANCA) in their serum. In addition, MPO was identified to be the antigen to MPO-ANCA using MPO-deficient mice.[9] These findings show the substances including β-glucan derived from *C. albicans* might relate to coronary arteritis.

The number of opportunistic infections is on the rise accompanying the proliferation of highly advanced medical treatment. *Candida* infections are frequently observed in patients in high-risk groups.[10,11] As the chemotherapeutic agent for mycoses is completely different from that for bacterial infections, early diagnosis is critical.[12,13] Since fungal cell wall contains β-glucan as its main component, β-glucan is detected in the blood of patients with deep mycoses. Thus, measurement of β-glucan in the blood is widely used for the early diagnosis of deep mycoses.[14,15] In this study, we cultured *Candida* spp. in completely synthetic media, obtained the water-soluble polysaccharide fraction released into the culture supernatant (*Candida albicans* water-soluble fraction or CAWS), and performed various analyses on that fraction. As a result, CAWS was found to be composed of mannoprotein and a β-glucan complex and to activate the limulus G factor, to exhibit acute lethal toxicity in the case of

intravenous administration, and to activate vascular endothelial cells, platelets and lymphocytes.[16-18] In addition to CADS, other substances in the soluble fraction may cause the development of coronary arteritis in mice.

In the present study, the incidence of coronaritis was found to be higher when CAWS was administered than when the conventional alkaline extract was administered, and a difference in the incidence was observed among mouse strains. We also analyzed the correlation of cytokine production in the development of coronary arteritis induced by CAWS.

MATERIALS AND METHODS

Mice

Male C3H/HeN and DBA/2 mice were purchased from Japan SLC, whereas male C57BL/6 and CBA/J mice were purchased from Charles River Japan. The mice were housed in a specific pathogen-free (SPF) environment and were used in the study at 5–14 weeks of age.

Organisms

Candida albicans strain IFO1385 was purchased from the Institute for Fermentation, Osaka (IFO), stored at 25°C on Sabauroud's agar (Difco, USA) and passaged once every three months.

Preparation of CAWS

CAWS was prepared from *C. albicans* strain IFO1385 in accordance with conventional methods.[18] The procedure used is as follows: 5 L of medium (C-limiting medium) was added to a glass incubator and cultured for 2 days at 27°C while supplying air at a rate of 5 L/min and rotating at 400 rpm. Following the culture, an equal volume of ethanol was added and after the mixture was allowed to stand overnight, the precipitate was collected. The precipitate was dissolved in 250 mL of distilled water, ethanol was added and the mixture was allowed to stand overnight. The precipitate was collected and dried with acetone to obtain CAWS.

Administration Schedule for Induction of Coronary Arteritis

CAWS (0 or 4 mg/mouse) was administered intraperitoneally for 5 consecutive days to each mouse in week 1. In week 5, CAWS (0 or 4 mg/mouse) was again administered in the same manner as that in week 1, after which the mice were sacrificed in week 9. The hearts of the animals were fixed with 10% neutral formalin and prepared in paraffin blocks. Tissue sections were stained with Hemotoxylin-Eosin (HE) stain. Cells were prepared from the spleen and cultured. Cells were also prepared from peritoneal exudative cells (PECs) and from the thymus, and enumerated. Liver weight was measured.

Preparation of Mouse Serum

The mice were anesthetized with chloroform and then sacrificed after which blood was drawn from the heart. After the blood samples had been left to stand for 60 minutes at room temperature and then for 60 minutes at 4°C, they were separated by centrifugation at 15,000 rpm × 10 minute, and the resulting supernatant was used as the serum. All the samples were stored at −25°C or lower.

CAWS-Specific Reaction in the Isolated Spleen Cells

The mice were anesthetized and then sacrificed, after which the spleen was excised. After teasing using a mesh in RPMI-1640 medium, the tissue was separated by centrifugation at 1200 rpm × 5 minute, and the resulting cells were treated with ACK-lysing buffer (NH_4Cl 8.20 g/L, $KHCO_3$ 1 g/L, EDTA·2Na 37.2 mg/L). After two washes with RPMI medium, the spleen cells were counted to adjust the cell density and then used after being suspended in RPMI medium with 10% FCS (fetal calf serum). The spleen cells were adjusted to 1×10^7 in RPMI 1640 medium containing 10% FCS and 500 µl aliquots were added to each well of a 48-well plate. Following the addition of CAWS (0, 2.5, 5 or 10 µg/ml), the cells were culture for 48 hours in a 5% CO_2 incubator at 37°C. The cytokine level of the culture supernatant was determined by Enzyme-Linked Immuno Sorbent Assay (ELISA) as described below.

Measurement of IL-1β, IL-4, IL-10 and IL-12

The IL-1β level was measured using a Mouse IL-1β ELISA Kit (Biosource International). Levels of IL-4, IL-10 and IL-12 were measured using Mouse IL-4, IL-10 and IL-12 $O_{PT}EIA^{TM}$ Kits (Pharmingen).

Measurement of IL-6

An ELISA 96-well plate (Sumitomo Bakelite) was coated with rat anti-mouse IL-6 mAb (Pharmingen) using 0.1 M bicarbonate buffer (pH 9.5) and incubated overnight at 4°C. After a wash with Phosphate buffered saline with 0.05% Tween 20 (PBST), the antibody was blocked for 40 minutes at 37°C with BPBST. This was followed by the addition of standard and sample (50 µL), incubation for 40 minutes at 37°C and washing with PBST. Fifty microliters of a secondary antibody in the form of biotinylated rat anti-mouse IL-6 mAb (1/2000; Pharmingen) was then added, and after incubation for 40 minutes at 37°C and a wash with PBST, peroxidase-conjugated streptavidin (1/10000; Zymed Laboratories, Inc.) was added. This was followed by incubation for 40 minutes at 37°C and washing with PBST. Subsequently, 50 µL of peroxidase substrate (TMB microwell peroxidase substrate system, KPL Inc.) was added to generate color, and absorbance was measured as previously described. Recombinant mouse IL-6 (Pharmingen) was used as the standard.

Measurement of IFN-γ

An ELISA 96-well plate (Sumitomo Bakelite) was coated with rat anti-mouse IFN-γ monoclonal antibody (mAb; Pharmingen) using 0.1 M $NaHCO_3$ (pH 8.2) and

incubated overnight at 4°C. After a wash with 0.05% Tween-PBS (PBST), the antibody was blocked for 40 minutes at 37°C with 0.5% BSA (bovine serum albumin)-PBST (BPBST). This was followed by the addition of standard and sample (50 μL), incubation for 40 minutes at 37°C and washing with PBST. Fifty microliters of a secondary antibody in the form of biotinylated rat anti-mouse IFN-γ (1/1000; Pharmingen) was then added, and after incubation for 40 minutes at 37°C and a wash with PBST, peroxidase-conjugated streptavidin (1/2000; Pharmingen) was added. This was followed by incubation for 40 minutes at 37°C and washing with PBST. Subsequently, color was generated using peroxidase substrate (TMB microwell peroxidase substrate system, KPL Inc.). After termination of the reaction with 1 M phosphoric acid, absorbance (OD 450/Ref. 630) was measured. Recombinant mouse IFN-γ (Pharmingen) was used as the standard.

Measurement of TNF-α

An ELISA 96-well plate (Nunc) was coated with rat anti-mouse TNF-α mAb (1/500; Pharmingen) using 0.1 M NaH_2PO_4– 0.1 M Na_2HPO_4 buffer (pH 6.0) and incubated overnight at 4°C. After a wash with PBST, the antibody was blocked for 60 minutes at room temperature with BPBST. This was followed by the addition of standard and sample (50 μL), incubation for 3 hours at room temperature and washing with PBST. Fifty microliters of a secondary antibody in the form of biotinylated rat anti-mouse TNF-α mAb (1/1000; Pharmingen) was then added, and after incubation for 60 minutes at room temperature and a wash with PBST, horseradish-peroxidase-conjugated streptavidin (1/1000; Pharmingen) was added. This was followed by incubation for 30 minutes at room temperature and washing with PBST. Subsequently, color was generated and absorbance was measured as previously described. Recombinant mouse TNF-α (Pharmingen) was used as the standard.

Measurement of Anti-CAWS Antibody Titer

An ELISA 96-well plate (Nunc) was coated with CAWS using 0.1 M bicarbonate buffer (pH 9.5) and incubated overnight at 4°C. After a wash with PBST, the antibody was blocked for 60 minutes at 37°C with BPBST and again washed with BPST. A serum sample diluted with BPBST (50 μl) was added, and incubation continued for another 60 minutes at 37°C. After a wash with PBST, 50 μL of peroxidase-conjugated goat anti-mouse IgG + IgM Ab (1/5000; Wako) was added and reaction was allowed to proceed for 60 minutes at 37°C. Color was generated and absorbance was measured as previously described. Furthermore, color generation was stopped after 10 minutes.

Measurement of Antibody Subclass

An ELISA 96-well plate (Nunc) was coated with CAWS using 0.1 M bicarbonate buffer (pH 9.5) and incubated overnight at 4°C. After a wash with PBST, the antibody was blocked for 60 minutes at 37°C with BPBST and again washed with PBST. A serum sample (50 μL) diluted with BPBST was added and incubation continued

for another 60 minutes at 37°C. After a wash with PBST, 50 μL of biotin-conjugated anti-mouse IgG1 (1/1000)-IgG2a (1/3000)-IgM (1/5000) Ab or peroxidase-conjugated anti-mouse IgE Ab (1/500) was added and the reaction was allowed to proceed for 60 minutes at 37°C. With respect to the biotin-conjugated antibody, after a wash with PBST, horseradish-peroxidase-conjugated streptavidin (1/5000; Pharmingen) was added, and incubation was continued for 60 minutes at 37°C. Color was generated and absorbance measured as previously described. Furthermore, color generation was stopped after 10 minutes.

Test for Significant Difference

Tests for significant differences in this study were performed using Student's t-test and values of $P<0.05$ were judged significant.

RESULTS

Development of Coronary Arteritis Induced with CAWS and Difference Among Strains

Administration of CAWS induced the development of coronary arteritis (Fig. 1). The arteritis-inducing activity of CAWS was compared among four mouse strains in accordance with the method of Murata et. al.[7,8] CAWS was dissolved in physiological saline to a concentration of 4 mg/0.2 mL, administered intraperitoneally to each mouse for five consecutive days, and again administered for five consecutive days in week 5, after which the mice were sacrificed in week 9. The tissue sections in the ninth week were prepared from the origin of the coronary arteries of the coronary aorta and stained with HE. The coronary arteritis induced by CAWS was accompanied by hypertrophy of the tunica intima, the rupture of elastic fibers and a diffuse invasion by lymphocytes, histiocytes, fibroblasts, smooth muscle cells and eosinophils of vascular endothelial cells and the regions surrounding blood vessels (Fig. 1). On the basis of such characteristics, the coronary arteritis induced by CAWS was presumed to be the so-called proliferative granulomatous coronary arteritis, and is clearly different from fibrinoid arteritis. Differences in the incidence of coronary arteritis were observed among the mouse strains. The coronary arteritis was observed in all mice of the DBA/2, C57BL/6 and C3H/HeN strains. It was observed to cover nearly the entire periphery of the vessels in DBA/2 mice, and those mice were considered to demonstrate the most virulent form of coronary arteritis (data not shown). On the other hand, CBA/J mice exhibited the lowest incidence of coronary arteritis among the four strains tested (10%), with few sites where coronary arteritis occurred.

Comparison of Survival Rates Among CAWS-Administered Mice

Among the mice administered CAWS according to the coronary arteritis induction protocol, only DBA/2 mice exhibited high mortality. Therefore, the disease

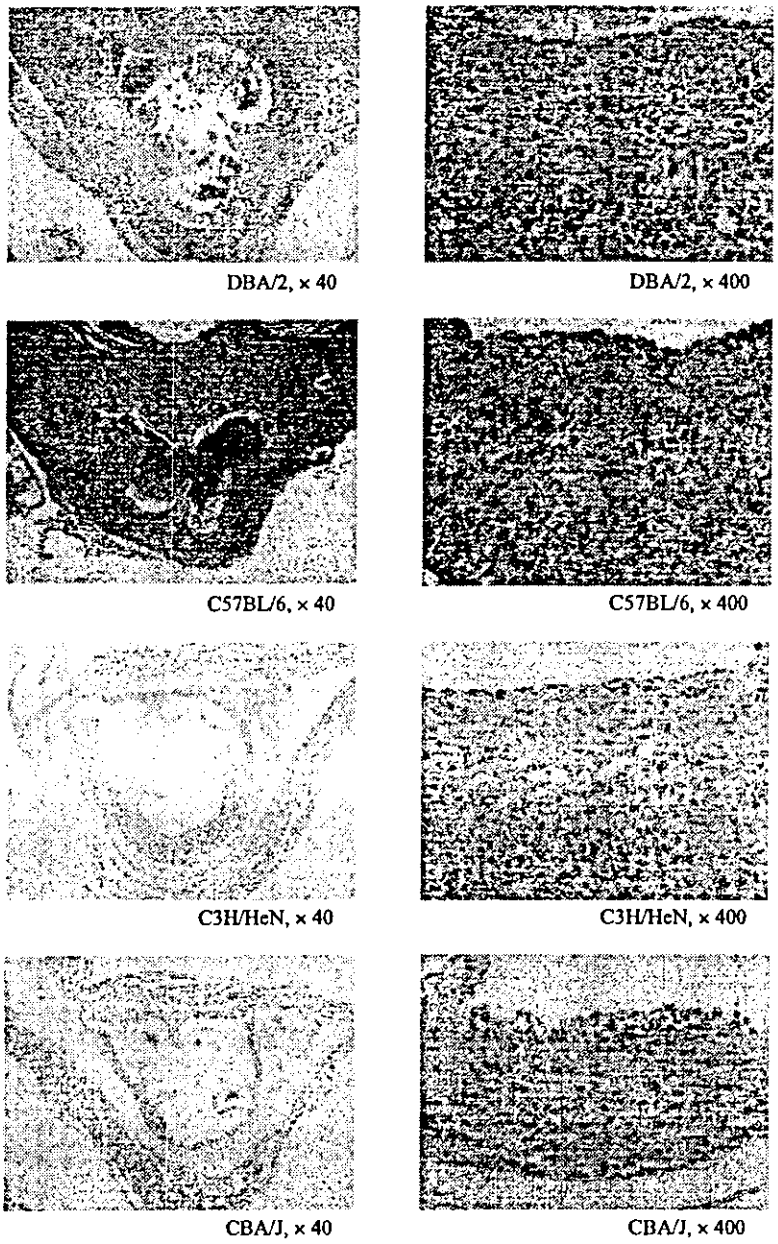

Figure 1. Histological observations of coronary arteritis. CAWS (4 mg/mouse) was administered i.p. to DBA/2, C57BL/6, C3H/HeN and CBA/J mice for five consecutive days in the 1st and 5th week. In the 9th week, mice were sacrificed and prepared sections stained with the hematoxylin-eosin method.

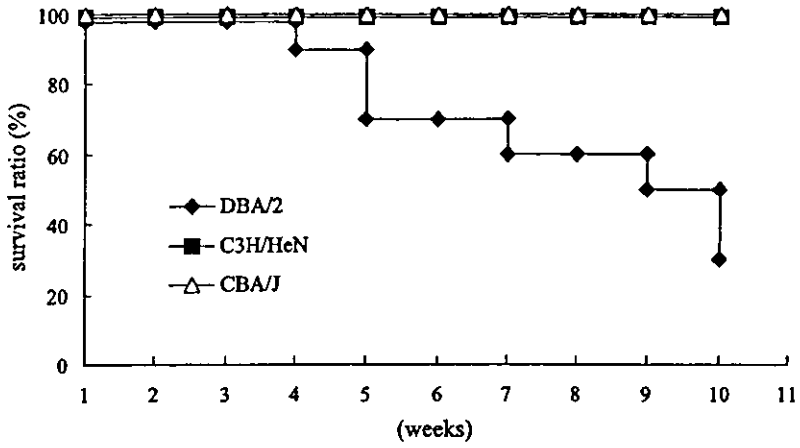

Figure 2. Survival ratio of CAWS-administered mice. CAWS (4 mg/mouse) was administered i.p. to DBA/2, C3H/HeN and CBA/J mice for five consecutive days in the 1st and 5th week. Survival had been observed for ten weeks. (N = 10).

course was examined in DBA/2 mice. DBA/2 mice were confirmed to expire beginning in the fourth week after the start of administration. The number that expired gradually increased and by the ninth week when the mice were assessed for coronary arteritis, the survival rate had dropped to 50%, and ultimately decreased to 30% (Fig. 2).

Tissue sections were prepared from the hearts of expired DBA/2 mice and observed microscopically using the HE stain. In the DBA/2 mice that expired due to administration of CAWS (n = 3), prominent neutrophil and histiocyte invasion was observed, along with the disappearance of striated muscle (Fig. 3A), and in some of the tissue, fibrosis appeared to occur in addition to cellular invasion (Fig. 3B and C); namely, the cause of death was suggested to be myocardial infarction. On the basis of these findings, it was suggested that the most virulent form of coronary arteritis was induced in DBA/2 mice, which resulted in the occurrence of cardiac ischemia that ultimately led to myocardial infarction.

Change of Cell Number in Organs on CAWS-Administration

As we observed a high incidence of cornory arteritis induced with CAWS in three strains, the increase in the numbers of immune cells was determined, along with the weight of the liver. These measurements were made in mice administered CAWS in accordance with the coronary arteritis induction protocol. In the spleen, although splenomegaly was observed in C3H/HeN, DBA/2 and C57BL/6 mice, significant increases in cell counts were exhibited by only C3H/HeN and DBA/2 mice (Fig. 4A). There were no changes in the thymus cell count in any mouse strains (Fig. 4B). In the case of PECs, although the changes were not significant, all strains exhibited an increase (Fig. 4C). There were no changes in liver weight (Fig. 4D).

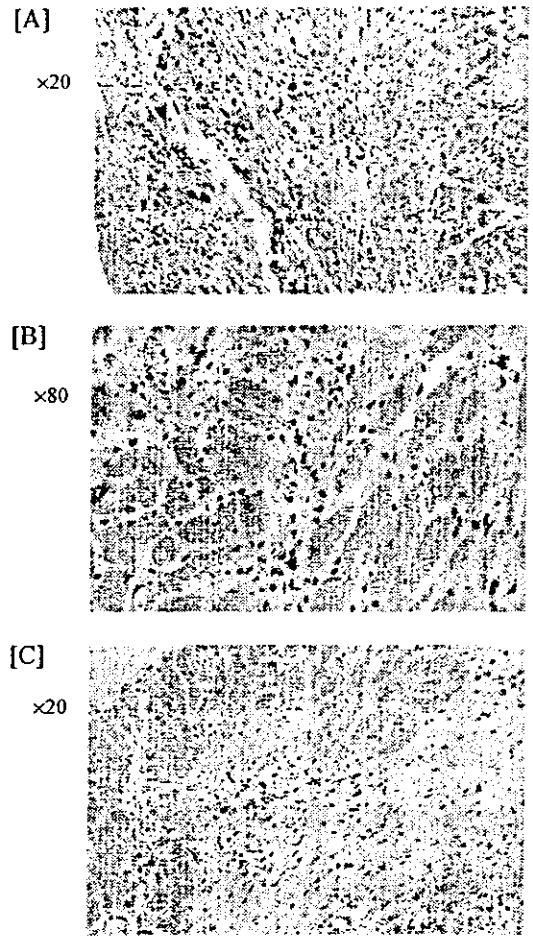

Figure 3. Histological analysis of dead DBA/2 mice administered with CAWS. [A, B, C] CAWS (4mg/mouse) was administered i.p. to DBA/2 mice for five consecutive days in the 1st and 5th week. Thereafter, the hearts of dead mice were stained with hematoxylin-eosin.

Cytokine Production by Spleen Cells of CAWS-Administered Mice on Stimulation with CAWS

As splenocyte counts in DBA/2 mice were high, we examined the production of cytokines in response to CAWS. Spleen cells of mice administered CAWS to induce coronary arteritis were prepared at a concentration of 1×10^7 cells/ml, and cultured for 48 hours in a 5% CO_2 incubator at 37° for observing cytokine production. Following the culture, IL-1β, IL-4, IL-6, IL-10, IL-12, IFN-α, and TNF-α levels in the culture supernatant were measured by ELISA. The strains with severe coronary arteritis, C3H/HeN, DBA/2 and C57BL/6 mice, showed IL-1β and IL-6 production by spleen cells in the CAWS -administered group (Fig. 5). In contrast, IL-10 was significantly produced

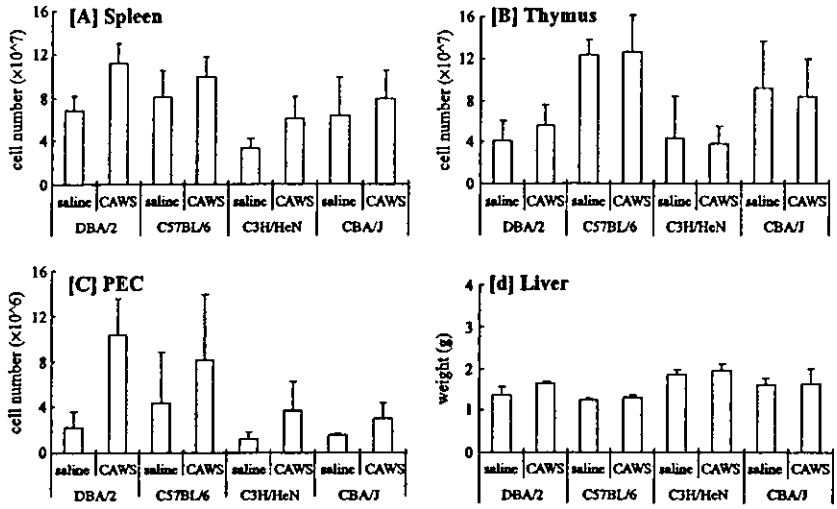

Figure 4. Cell number in peripheral blood and organ weight from CAWS-administered mice. CAWS (0 or 4mg/mouse) was administered i.p. to DBA/2, C57BL/6, C3H/HeN and CBA/J mice for five consecutive days in the 1st and 5th week. In the 9th week, the internal organs were collected from each mouse. Total cell number was counted with a hemocytometer and organ weight was measured with a analytical balance. The results show the mean ± standard deviation (S.D.). *; $P<0.05$ compared with the control using Student's *t-test*. [A]: Spleen, [B]: Thymus, [C]: PEC, [D]: Liver.

by spleen cells of the CBA/J mouse, which is the strain resistant to the coronary arteritis induced by CAWS.

In order to observe CAWS-specific reactions, the spleen cells of mice administered CAWS were stimulated with CAWS (0, 2.5, 5 or 10 μg/ml) and cultured for 48 hours in a 5% CO_2 incubator at 37°C. IFN-γ, IL-6 and IL-10 levels correlated well with the degree of coronary arteritis induced by CAWS (Fig. 6). IFN-γ and IL-6 production in DBA/2 and C57BL/6 mice tended to increase during the CAWS-specific response in the CAWS groups as compared with the saline groups, but no response was observed in C3H/HeN and CBA/J mice. IL-10 production was particularly enhanced in CBA/J mice treated with CAWS and slightly increased in the saline group, but no significant increase in production was observed even with the administration of CAWS in DBA/2 and C57BL/6 mice, and only a slight increase in C3H/HeN mice. Levels of other cytokines were not correlated with the coronary arteritis caused by CAWS. The amount of IL-4 production was small in all strains, but increased somewhat in CBA/J and C3H/HeN mice. IL-12 was hardly detected in any of the strains.

Measurement of Anti-CAWS Antibody Titer

Serum was obtained from mice administered CAWS in accordance with the coronary arteritis induction protocol, and anti-CAWS antibody in serum was detected with anti-mouse IgG + IgM Ab. Anti-CAWS antibodies were detected in all of the

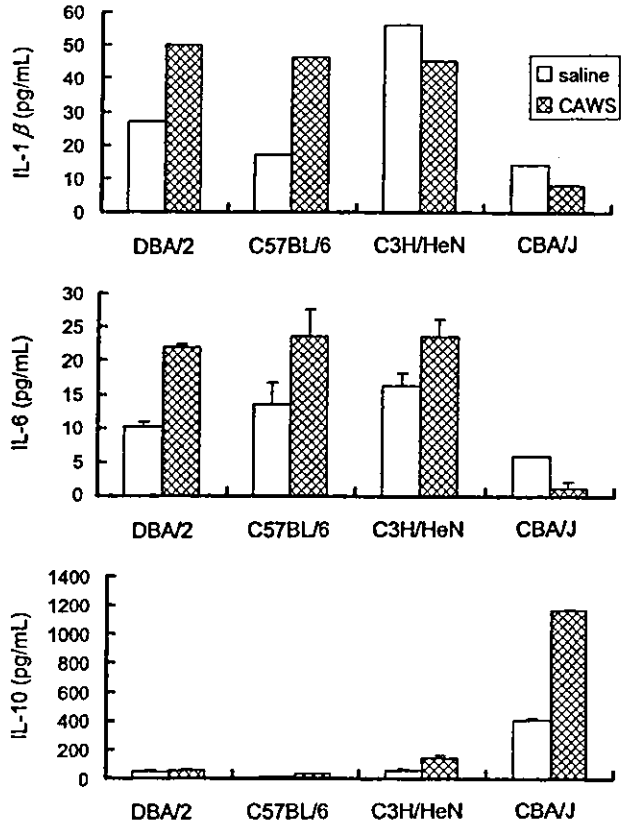

Figure 5. Cytokine production in culture supernatants of splenocytes in vivo from CAWS-administered mice. CAWS (0 or 4mg/mouse) was administered i.p. to DBA/2, C57BL/6, C3H/HeN and CBA/J mice for five consecutive days in the 1st and 5th week. In the 9th week, splenocytes were collected from each mouse. The splenocytes were cultured for 48 hour at a density of 1×10^7 cells/ml. The culture supernatants were collected and the level of each cytokine was measured by ELISA. The data shows one of four (C3H/HeN and CBA/J), three (DBA/2) or two (C57BL/6) experiments performed with similar results. The results show the mean ± standard deviation (S.D.).

mice, and the titers were extremely high (Fig. 7). Although the IgM titer varied depending on the mouse strain, there was no relationship between the IgM and the incidence of coronary arteritis (Fig. 8). Little IgE was detected in any of the strains. Conversely, IgG1 was detected at high levels in all the strains. CBA/J mice exhibited the lowest IgG2a titers.

On the basis of the above results, the antibodies produced in the form of anti-CAWS antibodies consisted mainly of IgG, followed by IgM. With respect to IgG2a production, although the titers were low in CBA/J and C57BL/6 mice, as the levels in CBA/J mice were roughly half those in C57BL/6 mice, and when considering the results of cytokine production in the spleen, it is possible that CBA/J mice exhibit Th2 bias.

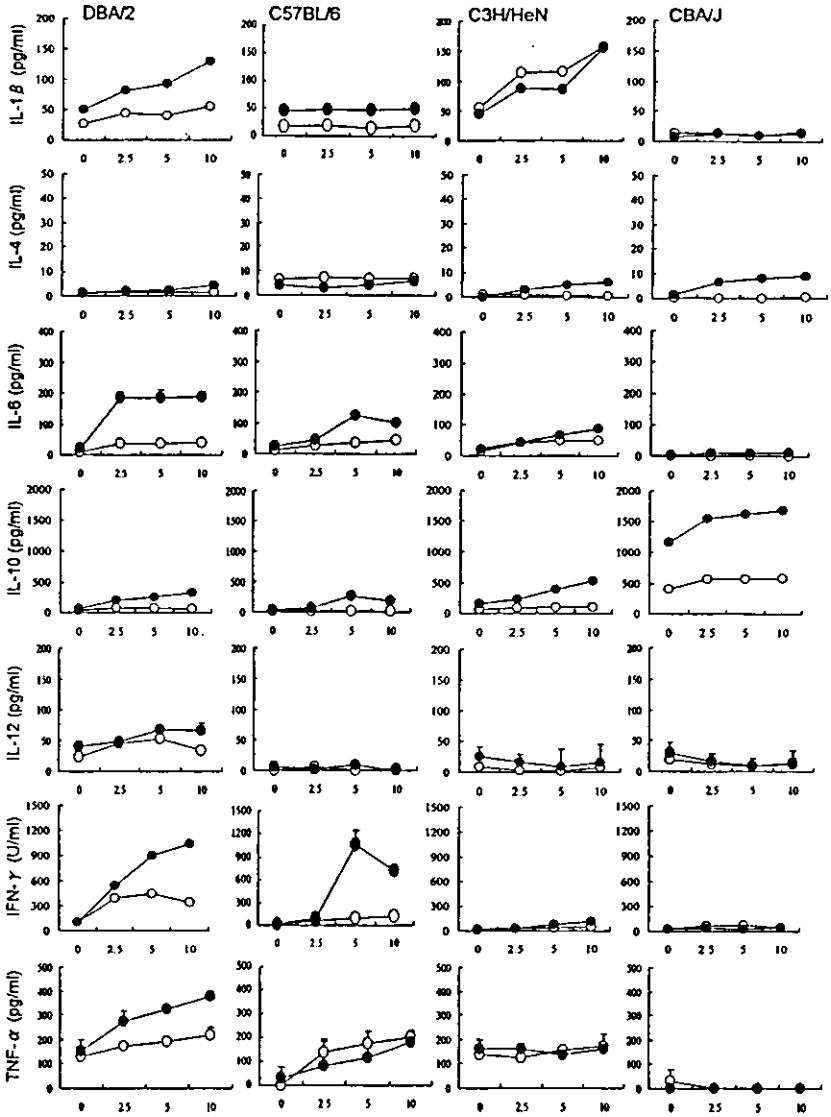

Figure 6. Cytokine production in culture supernatants of splenocytes stimulated with CAWS in vivo from CAWS-administered mice. CAWS (0 or 4mg/mouse) was administered i.p. to DBA/2, C57BL/6, C3H/HeN and CBA/J mice for five consecutive days in the 1st and 5th week. In the 9th week, splenocytes were collected from each mouse. The splenocytes were cultured with CAWS (0, 2.5, 5 or 10 μg/ml) for 48 hour at a density of 1×10^7 cells/ml. The culture supernatants were collected and the level of each cytokine was measured by ELISA. The data shows one of four (C3H/HeN and CBA/J), three (DBA/2) or two (C57BL/6) experiments performed with similar results. The results show the mean ± standard deviation (S.D.). *; $P < 0.05$ compared with the control using Student's *t-test*.

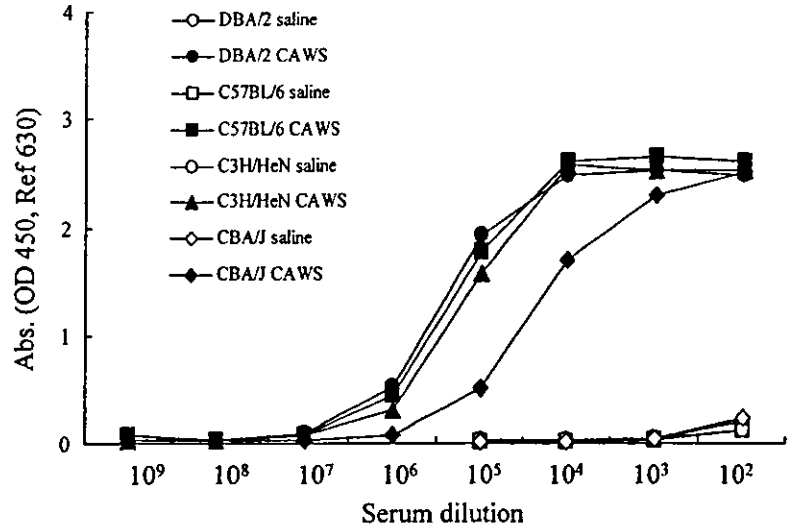

Figure 7. Anti-CAWS antibody in sera from CAWS-administered mice. CAWS (0 or 4mg/mouse) was administered i.p. to DBA/2, C57BL/6, C3H/HeN and CBA/J mice for five consecutive days in the 1st and 5th week. In the 9th week, sera were collected from each mouse. Anti-CAWS antibody was measured by ELISA. Color development was stopped after 10 min.

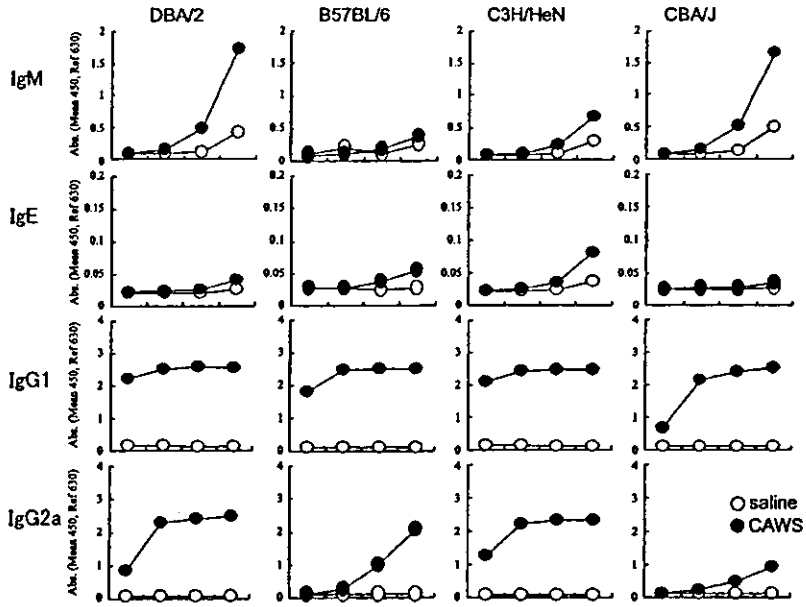

Figure 8. Immunoglobulin subclasses of anti-CAWS antibody in sera from CAWS-administered mice. CAWS (0 or 4mg/mouse) was administered i.p. to DBA/2, C57BL/6, C3H/HeN and CBA/J mice for five consecutive days in the 1st and 5th week. In the 9th week, sera were collected from each mouse. Anti-CAWS immunoglobulin subclasses were measured by ELISA. Color development was stopped after 10 minute.

DISCUSSION

Kawasaki disease is a febrile inflammatory disease that presents with systemic arteritis, and can be fatal particularly in the case of an exacerbation of coronaritis. When CAWS is administered to mice in accordance with the protocol of Murata et al.,[7,8] a Kawasaki-disease-like angiitis is induced at the origin of the coronary arteries. In the present study, strain differences were found to exist with respect to the incidence of the disease induced by CAWS with DBA/2, C3H/HeN and C57BL/6 mice exhibiting sensitivity and CBA/J mice exhibiting resistance. Moreover, histological observation of the sites of coronaritis in DBA/2 mice revealed hypertrophy of the tunica intima and cellular invasion, and the disease occurred with extremely high levels of severity and frequency. DBA/2 mice developed a much more severe coronary arteritis than the other strains. In addition, DBA/2 mice exhibited high mortality during the course of the disease's induction, and based on findings obtained from histological examination of the hearts, the cause of death was suspected to be myocardial infarction attributable to coronary occlusion. Because the difference in sensitivity to CAWS among the mouse strains examined in this study correlates strongly with the diversity of prognoses for Kawasaki disease patients,[19] this model is considered to be effective for elucidating the cause of coronary arteritis associated with Kawasaki disease, analyzing the characteristic condition, and developing more effective treatment methods.

Among patients with Kawasaki disease in the acute stage, cytokines, including IL-1, IL-2, IL-2 receptor, IL-6 and TNF-α, are detected in the serum.[20–23] When the production of cytokines from spleen cells was measured in mice stimulated with CAWS in vitro, a similar trend was demonstrated by the three strains that were sensitive to coronary arteritis induction, namely, DBA/2, C3H/HeN and C57BL/6, and in the case of DBA/2 mice in particular, a prominent CAWS-specific response involving inflammatory cytokines such as IL-6, IFN-γ and TNF-α, was observed, indicating the occurrence of an inflammatory immune response. The levels of inflammatory cytokines produced were high in DBA/2 mice in particular. On the other hand, an increased production of IL-10, which exhibits an immunosuppressive action, was observed in CBA/J mice that exhibited resistance to the occurrence of coronary arteritis. It is interesting to note that these cytokine production patterns resemble those observed in Kawasaki disease patients.

However, as there is one report indicating increased production of IL-4 and IL-10 in patients with Kawasaki disease,[24] dynamics that do not necessarily coincide with the findings of this study are observed. The discrepancies may be related to the stage of the disease (acute, subacute or recovery stage), thus indicating the need for further study of the relationship between cytokine production and the condition of Kawasaki disease.

Analyses have been conducted on the background genes of various diseases, and in the case of Kawasaki disease as well, there is a possibility of some form of involvement by genetic factors.[25,26] During the course of research on genes associated with coronaritis in rodents, numerous analyses have been conducted on the relationship between arteriosclerosis and hyperlipemia, and the IL-10 gene has been reported to have a close relationship with the lesions of coronary arteritis.[27,28] This finding also supports the findings obtained in the present study. In addition, although CBA is a strain derived from DBA, it is quite interesting that there are large differences in the

incidences of coronary arteritis and myocarditis induced by CAWS between the two strains. A survey of the genes involved in mouse coronaritis also suggested the existence of multiple inductive genes and repressor genes. This is a subject that requires detailed analysis.

On the basis of the above results, the activation of lymphocytes, vascular endothelial cells and so forth was prominently induced by means of hypercytokinemia in DBA/2 mice, and the resulting coronaritis promoted the occurrence of chronic myocardial ischemia, which, as a result, was thought to ultimately lead to death caused by fibrosis, infarction and cardiac insufficiency. It is hoped that this model will contribute not only to elucidation of the stage of Kawasaki disease and the associated coronary arteritis, but also to the improvement and development of treatment methods.

ACKNOWLEDGMENTS

This work was partly supported by a grant for private universities provided by Grant-in-Aid for Scientific Research, Ministry of Education, Culture, Sports, Science, and Technology and The Promotion and Mutual Aid Corporation for Private Schools, Japan.

REFERENCES

1. Kawasaki, T. Acute febrile muco-cutaneous lymph node syndrome in young children with unique digital desquamation. Jpn. J. Allergol. **1967**, *16*, 178–222.
2. Kawasaki, T.; Kosaki, F.; Okawa, S.; Shigematsu, I.; Yanagawa, H. New infantile acute febrile mucocutaneous lymph node syndrome (MLNS) prevailing in Japan. Pediatrics **1974**, *54*, 271–276.
3. Kato, H.; Ichinose, E.; Yoshioka, F.; Takechi, T.; Matsunaga, S.; Suzuki, K.; Rikitake, N. Fate of coronary aneurysms in Kawasaki disease: serial coronary angiography and long-term and follow-up study. Am. J. Cardiol. **1982**, *49*, 1758–1766.
4. Suzuki, A.; Kamiya, T.; Kuwahara, N.; Ono, Y.; Kohata, T.; Takahashi, O.; Kimura, K.; Takamiya, M. Coronary arterial lesions of Kawasaki disease: cardiac catheterization findings of 1100 cases. Pediatr. Cardiol. **1986**, *7*, 3–9.
5. Furusho, K.; Kamiya, T.; Nakano, H.; Kiyosawa, N.; Shinomiya, K.; Hayashidera, T.; Tamura, T.; Hirose, O.; Manabe, Y.; Yokoyama, T. High-dose intravenous gammaglobulin for Kawasaki disease. Lancet **1984**, *2*, 1055–1058.
6. Newburger, J.W.; Takahashi, M.; Beiser, A.S.; Burns, J.C.; Bastian, J.; Chung, K.J.; Colan, S.D.; Duffy, C.E.; Fulton, D.R.; Glode, M.P.; Mason, W.H.; Meissner, H.C.; Rowley, A.H.; Shulman, S.T.; Reddy, V.; Sundel, R.P.; Wiggins, J.W.; Colton, T.; Melish, M.E.; Rosen, F.S. A single intravenous infusion of gamma globulin as compared with four infusions in the treatment of acute Kawasaki syndrome. N. Engl. J. Med. **1991**, *324*, 1633–1639.
7. Murata, H.; Iijima, H.; Naoe, S.; Atobe, T.; Uchiyama, T.; Arakawa, S. The pathogenesis of experimental arteritis induced by Candida alkali-extract in mice. Jpn. J. Exp. Med. **1987**, *57*, 305–313.

8. Murata, H.; Naoe, S. Experimental Candida-induced arteritis in mice–relation to arteritis in Kawasaki Disease. Prog. Clin. Biol. Res. **1987**, *250*, 523.
9. Ishida-Okawara, A.; Oharaseki, T.; Takahashi, K.; Hashimoto, Y.; Aratani, Y.; Koyama, H.; Maeda, N.; Naoe, S.; Suzuki, K. Contribution of myeloperoxidase to coronary artery vasculitis associated with MPO-ANCA production. Inflammation **2001**, *25*, 381–387.
10. Holzheimer, R.G.; Dralle, H. Management of mycoses in surgical patients—review of the literature. Eur. J. Med. Res. **2002**, *7*, 200–226.
11. Ruffini, E.; Baldi, S.; Rapellino, M.; Cavallo, A.; Parola, A.; Robbiano, F.; Cappello, N.; Mancuso, M. Fungal infections in lung transplantation. Incidence, risk factors and prognostic significance. Sarcoidosis Vasc. Diffuse Lung Dis. **2001**, *18*, 181–190.
12. Alexander, B.D. Diagnosis of fungal infection: new technologies for the mycology laboratory. Transpl. Infect. Dis. **2002**, *4*, 32–37.
13. Marr, K.A. Antifungal prophylaxis in hematopoietic stem cell transplant recipient. Oncology **2001**, *15*, 15–19.
14. Obayashi, T.; Yoshida, M.; Mori, T.; Goto, H.; Yasuoka, A.; Iwasaki, H.; Teshima, H.; Kohno, S.; Horiuchi, A.; Ito, A.; Yamaguchi, H.; Shimada, K.; Kawai, T. Plasma (1→3)-β-D-glucan measurement in diagnosis of invasive deep mycosis and fungal febrile episodes. Lancet **1995**, *345*, 17–20.
15. Tamura, H.; Tanaka, S.; Ikeda, T.; Obayashi, T.; Hashimoto, Y. Plasma (1→3)-beta-D-glucan assay and immunohistochemical staning of (1→3)-beta-D-glucan in the fungal cell walls using a novel horseshoe crab protein (T-GBP) that specifically binds to (1→3)-beta-D-glucan. J. Clin. Lab. Anal. **1997**, *11*, 104–109.
16. Kurihara, K.; Shingo, Y.; Miura, N.N.; Horie, S.; Usui, Y.; Adachi, Y.; Yadomae, T.; Ohno, N. Effect of CAWS, a mannoprotein-beta-glucan complex of Candida albicans, on leukocyte, endothelial cell, and platelet functions in vitro. Biol. Pharm. Bull. **2003**, *26*, 233–240.
17. Uchiyama, M.; Ohno, N.; Miura, N.N.; Adachi, Y.; Yadomae, T. Anti-grifolan antibody reacts with the cell wall beta-glucan and the extracellular mannoprotein-beta-glucan complex of C. albicans. Carbohydr. Polym. **2002**, *48*, 333–340.
18. Uchiyama, M.; Ohno, N.; Miura, N.N.; Adachi, Y.; Aizawa, M.W.; Tamura, H.; Tanaka, S.; Yadomae, T. Chemical and immunochemical characterization of limulus factor G-activating substance of Candida spp.. FEMS Immunol. Med. Microbiol. **1999**, *24*, 411–420.
19. Hansaker, D.M.; Hunsaker, J.C., III; Adams, K.C.; Noonan, J.A.; Ackermann, D.M. Fatal Kawasaki disease due to coronary aneurysm rupture with massive cardiac tamponade. J. Ky. Med. Assoc. **2003**, *101*, 233–238.
20. Leung, D.Y.; Cotran, R.S.; Kurt-Jones, E.; Burns, J.C.; Newburger, J.W.; Pober, J.S. Endothelial cell activation and high interleukin-1 secretion in the pathogenesis of acute Kawasaki disease. Lancet **1989**, *2* (8675), 1298–1302.
21. Mancia, L.; Wahlstrom, J.; Schiller, B.; Chini, L.; Elinder, G.; D'Argenio, P.; Gigliotti, D.; Wigzell, H.; Rossi, P.; Grunewald, J. Characterization of the T-cell receptor V-beta repertoire in Kawasaki disease. Scand. J. Immunol. **1998**, *48*, 443–449.
22. Suzuki, H.; Uemura, S.; Tone, S.; Iizuka, T.; Koike, M.; Hirayama, K.; Madea, J. Effect of immunoglobulin and gamma-interferon on the production of tumor